Measurement-induced nonlocality in arbitrary dimensions in terms of the inverse approximate joint diagonalization

Li-qiang Zhang, Ting-ting Ma, and Chang-shui Yu*
School of Physics, Dalian University of Technology, Dalian 116024, China

(Received 17 October 2017; published 15 March 2018)

The computability of the quantifier of a given quantum resource is the essential challenge in the resource theory and the inevitable bottleneck for its application. Here we focus on the measurement-induced nonlocality and present a redefinition in terms of the skew information subject to a broken observable. It is shown that the obtained quantity possesses an obvious operational meaning, can tackle the noncontractivity of the measurement-induced nonlocality and has analytic expressions for pure states, $(2 \otimes d)$-dimensional quantum states, and some particular high-dimensional quantum states. Most importantly, an inverse approximate joint diagonalization algorithm, due to its simplicity, high efficiency, stability, and state independence, is presented to provide almost-analytic expressions for any quantum state, which can also shed light on other aspects in physics. To illustrate applications as well as demonstrate the validity of the algorithm, we compare the analytic and numerical expressions of various examples and show their perfect consistency.

DOI: 10.1103/PhysRevA.97.032112

I. INTRODUCTION

Quantum mechanical phenomena such as entanglement are not only fundamental properties of quantum mechanics, but also important physical resources due to their exploitation in quantum information processing tasks. Thus a mathematical quantitative theory, i.e., the resource theory (RT), is required to characterize the resource feature of these quantum phenomena. In recent years, the RT has been deeply developed for entanglement [1–6], quantum discord [7–12], quantum coherence [13–18], and so on [19,20]. However, as the core in RT, a good measure for the given resource of a general (especially high-dimensional) quantum state is only available for quantum coherence [13,21]. In contrast, quantum entanglement and quantum discord can be only well quantified in quite limited states [22–29]. Undoubtedly, their common challenge is the computability of the given measure (despite that, some conceptual questions, e.g., the entanglement measure of multipartite states, remain open). To study these quantum features, especially entanglement in a general (high-dimensional) quantum system, people usually have to seek the lower or upper bounds for the rough reference [5,30–32]. Comparably, an effective numerical way to evaluating a measure could be even more important for its potential applications in both the measure itself and the large-scale quantum system. For example, the conjugate-gradient method was proposed to calculate the bipartite entanglement of formation [33]; the semidefinite programming method was used to find the best separable approximation [34]; some numerical algorithms were developed for the evaluation of the relative-entropy entanglement of bipartite states [35,36,38]; 3-tangle was also evaluated by various numerical ways such as Monte Carlo methods [37], the conjugate-gradient method, and so on [38–40]; the local quantum uncertainty has been stably computed based on the approximate joint diagonalization algorithm [29]; and recently, numerical algorithms have also been used to calculate quantum coherence measures [41–44]. Generally speaking, a numerical algorithm depends not only on the question (the measure) but also on the state to be evaluated. In this sense, how to develop an effective algorithm for a particular quantum resource especially independent of the state is still of great practical significance.

In this paper, we present an effective numerical algorithm for the redefined measurement-induced nonlocality [45]. The measurement-induced nonlocality, dual to the quantum discord (to some extent) [7,8], is one type of nonlocality that characterizes the global disturbance on a composite state caused by the local nondisturbing measurement on one subsystem. However, the measurement-induced nonlocality, similar to geometric quantum discord [27,46], is originally defined based on the l_2 norm and inherits its noncontractivity, so it is not a good measure due to some unphysical phenomena that could be induced [47]. Although the measurement-induced nonlocality has been studied in many aspects [48–54], no obvious operational meaning has been found up to now and in particular, it can only be analytically calculated in low-dimensional quantum systems [45,51,52]. Here we will first redefine the measurement-induced nonlocality based on the skew information [55–57] in terms of the broken observable (a complete set of rank-one projectors) instead of a single observable. Thus not only the noncontractivity can be automatically solved, but also an obvious operational meaning related to quantum metrology has been found. Another distinct advantage of such a redefinition is that it can be analytically calculated for a large class of high-dimensional states and especially can induce a powerful numerical means, i.e., the inverse approximate joint diagonalization, to find an almost-analytic expression for any quantum state. It is shown that this algorithm can be stably and simply performed with even

*ycs@dlut.edu.cn

machine precision and especially it is state independent. The effectiveness of the algorithm is demonstrated by comparison with the analytic results of various examples.

The remainder of this paper is organized as follows. In Sec. II, we briefly introduce the measurement-induced nonlocality and present its new definition as well as its operational meaning. In Sec. III, we introduce the inverse approximate joint diagonalization algorithm and show how we convert the measurement-induced nonlocality to the standard optimization question governed by the the inverse approximate joint diagonalization. In Sec. IV, we demonstrate the power of the new definition and the algorithm in various applications. The conclusion is given in Sec. V.

II. MEASUREMENT-INDUCED NONLOCALITY BASED ON SKEW INFORMATION

A. Definition

To begin with, we briefly introduce the measurement-induced nonlocality [45] based on the l_2 norm. For a bipartite density matrix ρ_{AB}, the measurement-induced nonlocality is defined by the maximal disturbance of local projective measurements as

$$N(\rho_{AB}) = \max_{\Pi} \left\| \rho - \Pi^A(\rho_{AB}) \right\|_2^2, \tag{1}$$

where $\|\cdot\|_2$ denotes the l_2 norm of a matrix, and the von Neumann measurement Π^A is defined by $\sum_k (\Pi_k^A \otimes \mathbb{I}^B)\rho_{AB}(\Pi_k^A \otimes \mathbb{I}^B)$ with $\sum_k \Pi_k^A \rho_A \Pi_k^A = \rho_A$ guaranteeing that the reduced density matrix $\rho_A = \mathrm{Tr}_B \rho_{AB}$ is not disturbed. The measurement-induced nonlocality can be analytically calculated for two-qubit systems, but it is not contractive in that the measurement-induced nonlocality can be increased by some local operations on subsystem B and decreased by the tensor product of a third independent subsystem. To avoid noncontractivity, we can effectively utilize the properties of the skew information and directly present our definition of the measurement-induced nonlocality in the following rigorous way.

Definition 1. For an $(m \otimes n)$-dimensional density ρ_{AB}, the measurement-induced nonlocality can be defined in terms of skew information as

$$U(\rho_{AB}) = \max_{\{K_k\}} \sum_{k=0}^{m-1} I(\rho_{AB}, K_k), \tag{2}$$

where $I(\rho_{AB}, K_k) = -\frac{1}{2}\mathrm{Tr}[\sqrt{\rho_{AB}}, K_k]^2$ is the quantum skew information and $K_k = |k\rangle_A\langle k| \otimes \mathbb{I}_B$ with $|k\rangle$ denoting the eigenvectors of the reduced density matrix ρ_A.

At first, one can find that (i) $U(\rho_{AB}) = 0$ for any product state $\rho_{AB} = \rho_A \otimes \rho_B$; (ii) $U(\rho_{AB})$ is invariant under local unitary transformations; (iii) ρ_{AB} vanishes for any classical-quantum state $\rho_{AB} = \sum_k p_k |k\rangle_A\langle k| \otimes \rho_B$ with the nondegenerate reduced density matrix ρ_A; (iv) $U(\rho_{AB})$ is equivalent to the entanglement for pure ρ_{AB}, which can be found below from our Eq. (22). All the above properties of our redefined $U(\rho_{AB})$ are completely the same as the fundamental properties of the measurement-induced nonlocality given in Ref. [45]. This means that our $U(\rho_{AB})$ characterizes the same quantum resource as that in Ref. [45]. In addition, it is obvious that $U(\rho_{AB})$ is contractive and it is invariant under local unitary operations as a result of the good properties of the skew information. In addition, it can be found that the above definition of measurement-induced nonlocality has the obvious operational meaning related to quantum metrology.

B. Operational meaning

Let us consider a scheme of quantum metrology as follows. Suppose we have an $(m \otimes n)$-dimensional state ρ_{AB} with the reduced density matrix ρ_A and then let the state undergo a unitary operation $U_{\varphi_k} = e^{-iK_k\varphi_k}$ with $K_k = |k\rangle_A\langle k| \otimes \mathbb{I}_B$ and $[|k\rangle\langle k|, \rho_A] = 0$. This will endow an unknown phase φ_k to the state ρ_{AB} as $\rho_k = U_{\varphi_k}\rho_{AB}U_{\varphi_k}^\dagger$. We aim to estimate the measurement precision by measuring φ_k in ρ_k with $N >> 1$ runs of detection on ρ_k.

In the above scheme, the measurement precision of φ_k is characterized by the uncertainty of the estimated phase φ_k^{est} defined by

$$\delta\varphi_k = \left\langle \left(\frac{\varphi_k^{\mathrm{est}}}{\left|\partial\langle\varphi_k^{\mathrm{est}}\rangle/\partial\varphi_k\right|} - \varphi_k \right)^2 \right\rangle^{1/2}, \tag{3}$$

which for an unbiased estimator is just the standard deviation [58–60]. Based on the quantum parameter estimation [58–60], $\delta\varphi_k$ is limited by the quantum Cramér-Rao bound as $(\delta\varphi_k)^2 \geqslant \frac{1}{NF_{Qk}}$, where $F_{Qk} = \mathrm{Tr}\{\rho_\varphi L_\varphi^2\}$ is the quantum Fisher information with L_φ being the symmetric logarithmic derivative defined by $2\partial_\varphi\rho_\varphi = L_\varphi\rho_\varphi + \rho_\varphi L_\varphi$ [58]. It was shown in Refs. [58–60] that this bound can always be reached asymptotically by maximum likelihood estimation and a projective measurement in the eigenbasis of the "symmetric logarithmic derivative operator." Thus one can let $(\delta\varphi_k^o)^2$ denote the optimal variance which achieves the Cramér-Rao bound, i.e., $(\delta\varphi_k^o)^2 = \frac{1}{NF_{Qk}}$. Reference [61] showed that the Fisher information F_{Qk} is well bounded by the skew information as

$$\frac{F_{Qk}}{4} \leqslant 2I(\rho_{AB}, K_k) \iff \frac{1}{\left(\delta\varphi_k^o\right)^2} \leqslant 8NI(\rho_{AB}, K_k). \tag{4}$$

Suppose we repeat this scheme N times respectively corresponding to a complete set $\{K_k | [|k\rangle\langle k|, \rho_A] = 0\}$, we can sum Eq. (4) over k as

$$\sum_k \frac{1}{\left(\delta\varphi_k^o\right)^2} \leqslant 8N \sum_k I(\rho_{AB}, K_k) \leqslant 8NU(\rho_{AB}), \tag{5}$$

where the last inequality comes from Eq. (2). If we define $\frac{1}{(\Delta_\varphi^o)^2} = \sum_k \frac{1}{(\delta\varphi_k^o)^2}$, Eq. (5) can be rewritten as

$$\frac{1}{8NU(\rho_{AB})} \leqslant (\Delta_\varphi^o)^2, \tag{6}$$

which shows that the measurement-induced nonlocality $U(\rho_{AB})$ contributes to the lower bounds of the "average variance" $(\Delta_\varphi^o)^2$ that characterizes the contributions of all the inverse optimal variances of the estimated phases. It is worth emphasizing that $(\Delta_\varphi^o)^2$ *corresponds to an arbitrary complete set* $\{K_k | [|k\rangle\langle k|, \rho_A] = 0\}$ *instead of the optimal set in the sense of Eq. (2).* In addition, in the above mentioned asymptotical and the optimal regimes, Eq. (6) for the pure states (or incoherent states) will become $\frac{1}{4NU(\rho_{AB})} = (\Delta_\varphi^o)^2$ due to the

inequality $\frac{F_{Qk}}{4} \geqslant I(\rho_{AB})$ [61]. However, one can recognize that in the practical scenario, $\delta\varphi_k \geqslant \delta\varphi_k^o$ because the measurement protocol could not be optimal. Thus, it is immediately obtained that

$$\sum_k \frac{1}{(\delta\varphi_k)^2} \leqslant 8NU(\rho_{AB}) \iff \frac{1}{8NU(\rho_{AB})} \leqslant (\Delta_\varphi)^2, \quad (7)$$

with $\frac{1}{(\Delta_\varphi)^2} = \sum_k \frac{1}{(\delta\varphi_k)^2}$. Finally, we would like to emphasize that Eqs. (7) and (6) provide only the lower bound instead of the exact value of the "average variance" $(\Delta_\varphi)^2$ or $(\Delta_\varphi^o)^2$, because the inequalities are not saturated in the general cases. In this sense, our measurement-induced nonlocality was endowed with the operational meaning.

III. EFFECTIVE NUMERICAL ALGORITHM AND MEASUREMENT-INDUCED NONLOCALITY IN ARBITRARY DIMENSION

A. Approximate joint diagonalization algorithm

To give our main inverse approximate joint diagonalization algorithm, we first introduce the well-known approximate joint diagonalization algorithm [62–64] and its relevant approximate joint diagonalization optimization problem. For m n-dimensional matrices $\{M_m\}$, one aims to find a unitary matrix U such that

$$J(U) = \max_U \sum_{i=1}^{m} \sum_{k=1}^{n} |U M_i U^\dagger|_{kk}^2. \quad (8)$$

Such an optimization problem is a standard expression of the approximate joint diagonalization of the series of matrices M_i. This approximate joint diagonalization problem is widely met in the blind source separation and independent component analysis (see Ref. [65] and the references therein) and is well solved numerically by many effective algorithms. A very remarkable algorithm is the Jacobi method [62,63,65] which can be performed as steadily, reliably, fast, and perfectly as the diagonalization of a single matrix. The main idea of the approximate joint diagonalization algorithm of our interest is as follows.

Any unitary matrix U can be decomposed into a series of unitary matrices called Givens rotations as $U = \Pi_{\{\theta,\phi\}} U(\theta,\phi)$ with

$$U(\theta,\phi) = \begin{pmatrix} \cos\theta & e^{i\varphi}\sin\theta \\ -e^{-i\varphi}\sin\theta & \cos\theta \end{pmatrix}. \quad (9)$$

Each Givens rotation is only operated on the (2×2)-dimensional subspace of the m M_i's. Let

$$G_i = \begin{pmatrix} a_i & b_i \\ c_i & d_i \end{pmatrix} \quad (10)$$

denote the (2×2)-dimensional block matrix of M_i corresponding to the Givens rotation $U(\theta,\phi)$. After the Givens rotation, G_i is updated by

$$G_i' = U^\dagger(\theta,\phi) G_i U(\theta,\phi) = \begin{pmatrix} a_i' & b_i' \\ c_i' & d_i' \end{pmatrix}. \quad (11)$$

In this (2×2)-dimensional subspace, the optimization problem of Eq. (8) is equivalent to the problem

$$\max\{|a_i'|^2 + |d_i'|^2\} = \max\left\{\tfrac{1}{2}|a_k' - d_k'|^2 + \tfrac{1}{2}|a_k' + d_k'|^2\right\}, \quad (12)$$

by choosing suitable parameters θ and φ. Since the trace of a matrix is preserved under the unitary operations, i.e., $a_k' + d_k' = a_k + d_k$, the optimization problem of Eq. (13) is equivalent to

$$Q = \max \sum_{i=1}^{m} |a_k' - d_k'|^2, \quad (13)$$

which can be rewritten as [63]

$$Q = \max \frac{v^\intercal \mathrm{Re}(G^\dagger G) v}{v^\intercal v}, \quad (14)$$

where $G = [g_1, g_2, \ldots, g_m]$, $g_k = [a_k - d_k, b_k + c_k, i(c_k - b_k)]^\intercal$, $v = [\cos 2\theta, -\sin 2\theta \cos\varphi, -\sin 2\theta \sin\varphi]^\intercal$. The optimization problem maximizing Q in Eq. (14) happens to be the well-known Rayleigh quotient which shows that Q has a closed form and is just the maximal eigenvalue of the matrix $\mathrm{Re}(G^\dagger G)$. The eigenvector for the maximal eigenvalue achieves the optimization solution, by which one can solve the corresponding (θ,ϕ) and further find the optimal Givens rotation $U(\theta,\phi)$.

When all (2×2)-dimensional block matrices in M_i are updated once by the Givens rotations, it is called one sweep. Following the same procedure, each sweep transfers the contribution of the off-diagonal entries to the diagonal entries as required by optimization problem (8). The sweep is performed again and again until the required precision is reached.

B. Inverse approximate joint diagonalization algorithm

The inverse approximate joint diagonalization algorithm is completely parallel with the approximate joint diagonalization algorithm. Let us consider an inverse problem opposite to the problem in Eq. (8), namely, finding a proper unitary operation U such that

$$\tilde{J}(U) = \min_U \sum_{i=1}^{m} \sum_{k=1}^{n} |U M_i U^\dagger|_{kk}^2. \quad (15)$$

Following the completely same procedure as the approximate joint diagonalization algorithm, we can finally arrive at

$$\tilde{Q} = \min \frac{v^\intercal \mathrm{Re}(G^\dagger G) v}{v^\intercal v}. \quad (16)$$

Based on the Rayleigh quotient, $\tilde{Q}$, dual to Q, is just the minimal eigenvalue of the matrix $\mathrm{Re}(G^\dagger G)$. That is, $\tilde{J}(U)$ can be completely solved if we replace the maximal eigenvalue in the approximate joint diagonalization algorithm by the minimal eigenvalue. This is the inverse approximate joint diagonalization algorithm.

Based on the above algorithms, one can always find the optimal unitary operation U subject to a satisfactory precision. Corresponding, one can calculate the exact value of $\tilde{J}(U)$ or $J(U)$. For a neat formulation, we would like to give another definition.

Definition 2. The *inverse joint diagonalizer* of m matrices M_i is defined by U_o which is the optimal unitary

operation that achieves the aim of Eq. (15), i.e., $\tilde{J}(U) = \min_{U_0} \sum_{i=1}^{m} \sum_{k=1}^{n} |U_o M_i U_o^\dagger|_{kk}^2$. The *inverse joint eigenvalue* of M_i is defined by $\tilde{\lambda}_k^i = [U_o M_i U_o^\dagger]_{kk}$.

C. Measurement-induced nonlocality for arbitrary quantum states

Based on Definition 2, we can present our main theorem as follows.

Theorem 1. For an $(m \otimes n)$-dimensional state ρ_{AB}, define the matrices $A_{ij} = (\mathbb{I}_m \otimes \langle\psi_i|)\sqrt{\rho_{AB}}(\mathbb{I}_m \otimes |\psi_j\rangle)$ with $\{|\psi_i\rangle\}$ denoting any orthonormal basis of subsystem B. Then the measurement-induced nonlocality $U(\rho_{AB})$ of ρ_{AB} can be given by

$$U(\rho_{AB}) = 1 - \sum_{i,j=0}^{n-1} \left\{ \sum_{k=1}^{N} |\Phi_N^\dagger A_{ij} \Phi_N|_{kk}^2 + \sum_{\alpha} \sum_{k=1}^{D_\alpha} \left|\tilde{\lambda}_k^{\alpha ij}\right|^2 \right\}, \tag{17}$$

where $\Phi_N = [|1\rangle, |2\rangle, \ldots, |N\rangle]$ is the matrix made up of all the nondegenerate eigenvectors $\{|k\rangle\}$ of the reduced density matrix $\rho_A = \mathrm{Tr}_B\, \rho_{AB}$, $\Phi_{D_\alpha} = [|1\rangle_\alpha, |2\rangle_\alpha, \ldots, |D\rangle_\alpha]$ is the matrix made up of all the eigenvectors in the αth degenerate subspace of ρ_A with $N + \sum_\alpha D_\alpha = m$, and $\tilde{\lambda}_k^{\alpha ij}$ is the kth inverse joint eigenvalue of the matrix $\Phi_{D_\alpha}^\dagger A_{ij} \Phi_{D_\alpha}$.

Proof. From Eq. (2), we can find

$$\begin{aligned} U(\rho_{AB}) &= \max_{K_k} \sum_{k=0}^{m-1} \left[\mathrm{Tr}\rho_{AB} K_k^2 - \mathrm{Tr}\sqrt{\rho_{AB}} K_k \sqrt{\rho_{AB}} K_k \right] \\ &= 1 - \min_{K_k} \sum_{k=0}^{m-1} \mathrm{Tr}\sqrt{\rho_{AB}} K_k \sqrt{\rho_{AB}} K_k. \end{aligned} \tag{18}$$

Substituting $K_k = |k\rangle\langle k| \otimes \mathbb{I}$ with $\{|k\rangle\}$ denoting the eigenvectors of the reduced density matrix ρ_A and any orthonormal bases $\{|\psi_i\rangle\}$ of subsystem B into Eq. (18), it follows that

$$\begin{aligned} U(\rho_{AB}) &= 1 - \min_{\{|k\rangle\}} \sum_{i,j=0}^{n-1} \sum_{k=0}^{m-1} \mathrm{Tr}\sqrt{\rho_{AB}} (|k\rangle\langle k| \otimes |\psi_i\rangle\langle\psi_i|) \\ &\quad \times \sqrt{\rho_{AB}} (|k\rangle\langle k| \otimes |\psi_j\rangle\langle\psi_j|) \\ &= 1 - \min_{\{|k\rangle\}} \sum_{i,j=0}^{n-1} \sum_{k=0}^{m-1} |\langle k| A_{ij} |k\rangle|^2, \end{aligned} \tag{19}$$

with $A_{ij} = (\mathbb{I}_m \otimes \langle\psi_i|)\sqrt{\rho_{AB}}(\mathbb{I}_m \otimes |\psi_j\rangle)$. Suppose that the reduced density matrix ρ_A has N nondegenerate eigenvalues and α degenerate subspace with the dimension denoted by D_α, respectively, then one can always construct an $(m \times N)$-dimensional matrix Φ_N as $\Phi_N = [|1\rangle, |2\rangle, \ldots, |N\rangle]$ with the column $|k\rangle$ including all the nondegenerate eigenvectors of ρ_A and α $(m \times D)$-dimensional matrices Φ_{D_α} as $\Phi_{D_\alpha} = [|1\rangle_\alpha, |2\rangle_\alpha, \ldots, |D\rangle_\alpha]$ with the column $|k\rangle_\alpha$ covering all the eigenvectors in the αth degenerate subspace of ρ_A. It is obvious that $N + \sum_\alpha D_\alpha = m$. Thus the optimization of $\{|k\rangle\}$ in Eq. (19) is converted to the optimization of Φ_N and Φ_{D_α}. However, Φ_N is made up of the nondegenerate eigenvectors of ρ_A, so Φ_N is uniquely determined by ρ_A. As a result, only the optimization of Φ_{D_α} is required, since Φ_{D_α} is not unique in the degenerate subspace. If we denote any two different such matrices as Φ_{D_α} and Ψ_{D_α}, there always exists a unitary transformation as $\Psi_{D_\alpha} = \Phi_{D_\alpha} U$. So the optimization of Φ_{D_α} is essentially converted to the optimization of the unitary operations U once one fixes a representation (a particular Φ_{D_α}). Thus Eq. (19) can be rewritten as

$$U(\rho_{AB}) = 1 - \sum_{i,j=0}^{n-1} \sum_{k=1}^{N} |\Phi_N^\dagger A_{ij} \Phi_N|_{kk}^2 - \sum_{\alpha} \tilde{J}_\alpha(U_\alpha), \tag{20}$$

with

$$\tilde{J}_\alpha(U_\alpha) = \min_{U_\alpha} \sum_{i,j=0}^{n-1} \sum_{k=1}^{D_\alpha} |U_\alpha^\dagger \Phi_{D_\alpha}^\dagger A_{ij} \Phi_{D_\alpha} U_\alpha|_{kk}^2. \tag{21}$$

It is obvious that Eq. (21) is the standard inverse approximate joint diagonalization problem of matrices $\Phi_{D_\alpha}^\dagger A_{ij} \Phi_{D_\alpha}$ given in Eq. (15) which can be well solved by the inverse approximate joint diagonalization algorithm. Let $\lambda_k^{\alpha ij}$ denote the kth inverse joint eigenvalue of the matrix $\Phi_{D_\alpha}^\dagger A_{ij} \Phi_{D_\alpha}$, then Eq. (20) exactly becomes Eq. (17) in our main theorem, which completes our proof. ■

D. Efficiency of the inverse approximate joint diagonalization algorithm and the closure of the measurement-induced nonlocality

From the approximate joint diagonalization and inverse approximate joint diagonalization algorithms in the above section, one can find that the two algorithms have equal efficiency within the same precision. It is especially noted that the approximate joint diagonalization algorithm for a single matrix is exactly the Jacobi method for the diagonalization of a single matrix [66]. In this sense, we can safely conclude that the inverse approximate joint diagonalization algorithm has the same efficiency as the Jacobi method if they are executed for the same dimensional matrix subject to the same precision. Now let us consider the inverse approximate joint diagonalization algorithm in our measurement-induced nonlocality for an $(m \otimes n)$-dimensional density matrix ρ_{AB}. It is equivalent to the inverse approximate joint diagonalization of n^2 $(m \times m)$-dimensional matrices A_{ij} in the worst case (the reduced matrix is a maximally mixed state). Thus one can find that one sweep needs $\frac{m(m-1)}{2}$ Givens rotations and $\frac{m^2n^2 - mn^2}{2}$ unitary transformations (Givens rotation operations). However, if one diagonalizes ρ_{AB} with the Jacobi method, one will require $\frac{mn(mn-1)}{2}$ Givens rotations and an equal number of unitary transformations. It is obvious that under the same conditions, the inverse approximate joint diagonalization algorithm requires much fewer Givens rotations and unitary transformations than the Jacobi method for the diagonalization of ρ_{AB} especially for large n, which shows the high efficiency of the inverse approximate joint diagonalization algorithm. In particular, it was said that about $\log(m)$ sweeps were needed for a single matrix M_i subject to an acceptable precision (examples show around 10^{-16} in [66]).

In addition, one always expects a closed form (or an analytic expression) of a quantifier. This could be, in principle, achieved if the quantifier could be given in terms of the eigenvalues of some matrices, since the eigenvalues can be completely

determined by the secular equation of the matrix no matter whether they can be exactly calculated or not. However, in the practical scenario, the exact eigenvalues of a matrix can never be obtained, especially for the high-dimensional case. Thus a numerical algorithm is inevitable, which will have to lead to the practical broken closure. In other words, in the practical case, our inverse joint eigenvalues used above have equal weight as the eigenvalues of some matrices. In this sense, we emphasize that our expression in theorem 1 is almost analytic (or of closed form).

IV. EXAMPLES AND POWER OF THE INVERSE APPROXIMATE JOINT DIAGONALIZATION ALGORITHM

Next, we give some examples to verify the effectiveness of theorem 1 by comparing the strictly analytic expression and the numerical ones in theorem 1. All the examples show perfect consistency and prove the efficiency and superiority of theorem 1, especially in the high-dimensional case.

1. *Bipartite pure states*

Any bipartite pure state can be given in the Schmidt decomposition as $|\chi\rangle_{ab} = \sum_i u_i |ii\rangle_{ab}$ where u_i is the Schmidt coefficients. The measurement-induced nonlocality can be easily obtained as

$$\begin{aligned} U(\rho_{ab}) &= 1 - \min_{K_k} \sum_{k=0}^{n-1} \mathrm{Tr}(\sqrt{\rho_{AB}} K_k \sqrt{\rho_{AB}} K_k) \\ &= 1 - \min_{\{|k\rangle\}} \sum_{k=0}^{n-1} \left| \sum_{ij} u_i u_j \langle ii | (|k\rangle\langle k| \otimes \mathbb{I}_B) |jj\rangle_{AB} \right|^2 \\ &= 1 - \min_{\{|k\rangle\}} \sum_{k=0}^{n-1} \left| \sum_{i} u_i^2 \langle k|i\rangle \langle i|k\rangle_A \right|^2 \\ &= 1 - \sum_{k=0}^{n-1} u_k^4 = 1 - \mathrm{Tr}\rho_A^2, \end{aligned} \tag{22}$$

with the optimum value attained by $\langle k||i\rangle = \frac{1}{\sqrt{n}}$. It is explicit that the measurement-induced nonlocality for a pure state is exactly half of its entanglement in terms of the linear entropy of the reduced density matrix. To further validate our numerical procedure in theorem 1, we plot Eq. (22) and its corresponding numerical results for many pure states randomly generated by MATLAB R2017a in Fig. 1(a), which shows our numerical results are completely consistent with Eq. (22).

2. *Qubit-qudit states*

For a $(2 \otimes d)$-dimensional quantum state ρ_{AB} with the reduced density matrix ρ_A, the measurement-induced nonlocality can be given by

$$\begin{aligned} U(\rho_{AB}) &= -\frac{1}{2} \max_{[K_k,\rho_A]=0} \sum_{k=0}^{1} \mathrm{Tr}[\sqrt{\rho_{AB}}, K_k]^2 \\ &= - \max_{[K_k,\rho_A]=0} \mathrm{Tr}[\sqrt{\rho_{AB}}, K_0]^2. \end{aligned} \tag{23}$$

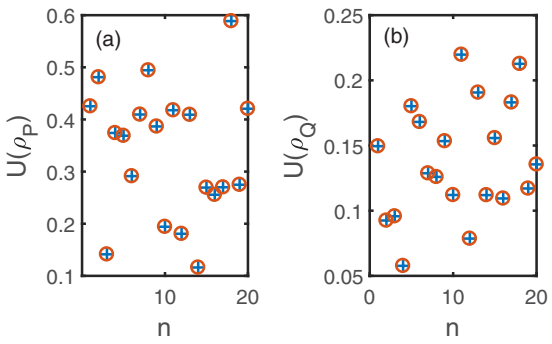

FIG. 1. Measurement-induced nonlocalities vs n. We calculated (a) 20 $(3 \otimes 3)$-dimensional pure states and (b) 20 $(2 \otimes 4)$-dimensional qubit-qudit mixed states randomly generated by MATLAB R2014b. Here n denotes the nth density matrix. The O stands for the strictly analytical expressions given by Eq. (22) for (a) and Eq. (24) for (b) and the + marks the numerical expressions given by Eq. (17) in both figures. Both show the perfect consistency.

In the qubit subsystem, the observable K_0 can be expanded in the Bloch representation as $K_0 = \frac{1}{2}(\mathbb{I}_2 + \vec{n}\cdot\vec{\sigma}) \otimes \mathbb{I}_d$ and ρ_A can be expanded as $\rho_A = \frac{1}{2}(\mathbb{I}_2 + \vec{r}\cdot\vec{\sigma}) \otimes \mathbb{I}_d$, where $\vec{n}$ with $\|\vec{n}\|_2 = 1$ and $\vec{r}$ with $\|\vec{r}\|_2 \leqslant 1$ denote the Bloch vector. Thus the optimization condition $[K_k, \rho_A] = 0$ is equivalent to $\vec{r}\times\vec{n} = 0$ and Eq. (23) arrives at

$$\begin{aligned} U(\rho_{AB}) &= \frac{1}{2} - \frac{1}{2} \min_{\vec{n}} \sum_{ij} \mathrm{Tr} n_i T_{ij} n_j \\ &= \begin{cases} \frac{1}{2}(1 - v_{\min}), & \vec{r} = 0, \\ \frac{1}{2}\left(1 - \frac{1}{\|\vec{r}\|_2^2} \vec{r}^T T \vec{r}\right), & \vec{r} \neq 0, \end{cases} \end{aligned} \tag{24}$$

where $v_{\min}$ is the minimal eigenvalue of the matrix T with $T_{ij} = \mathrm{Tr}\sqrt{\rho_{AB}}(\sigma_i \otimes \mathbb{I}_n)\sqrt{\rho_{AB}}(\sigma_j \otimes \mathbb{I}_n)$. Equation (24) gives the closed form of the measurement-induced nonlocality. Similar to case 1, we also plot the numerical measurement-induced nonlocality for the randomly generated qubit-qudit states in Fig. 1(b) which also validates our numerical results of theorem 1.

3. *$(3 \otimes 3)$-dimensional PPT states*

The $(3 \otimes 3)$-dimensional positive-partial-transpose (PPT) states [67] can be given by

$$\rho_{\mathrm{PPT}} = \frac{2}{7}|\Phi\rangle_3\langle\Phi| + \frac{\alpha}{7}\rho_+ + \frac{5-\alpha}{7}\rho_-, \quad \alpha \in [2,4], \tag{25}$$

where $|\Phi\rangle_m = \frac{1}{\sqrt{m}} \sum_{k=0}^{m-1} |kk\rangle$, and $\rho_+ = \frac{1}{3}\sum_{k=0}^{2} |k,k\oplus 1\rangle\langle k,k\oplus 1|$ and $\rho_- = \frac{1}{3}\sum_{k=0}^{2} |k\oplus 1,k\rangle\langle k\oplus 1,k|$ with $\oplus$ the modulo-3 addition. The parameter α determines the different quantum correlations of the PPT state. If $\alpha \leqslant 3$, ρ_{PPT} is separable. When $\alpha \in [3,4]$, the PPT state is entangled. But if $4 \leqslant \alpha \leqslant 5$, ρ_{PPT} is not a PPT state, but a free entangled state. Based on our definition 1, one can find that $U(\rho_{AB})$ can be analytically calculated for $\alpha \in [2,5]$ as

$$U(\rho_{\mathrm{PPT}}) = \begin{cases} \frac{21 - \sqrt{6(5-\alpha)} - \sqrt{6\alpha - 3\sqrt{\alpha(5-\alpha)}}}{31.5}, & N_T < \alpha \leqslant 5, \\ \frac{4}{21}, & 2 \leqslant \alpha \leqslant N_T, \end{cases} \tag{26}$$

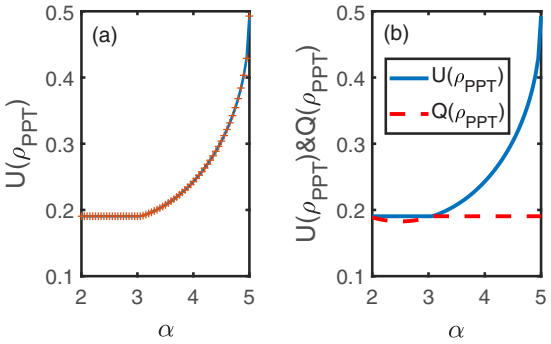

FIG. 2. (a) Measurement-induced nonlocality $U(\rho_{\rm PPT})$ for PPT states vs α. The solid line and the + line correspond to the strictly analytical expression of Eq. (26) and the numerical expression of Eq. (17). The sudden change point of the measurement-induced nonlocality is about $\alpha \approx 3.0669$. The measurement-induced nonlocality is invariant for $\alpha \leqslant 3.0669$, but becomes increasing for $\alpha > 3.0669$. (b) Comparison of the LQU $Q(\rho_{\rm PPT})$ and the measurement-induced nonlocality $U(\rho_{\rm PPT})$ based on PPT states. The solid line stands for $U(\rho_{\rm PPT})$, while the dotted line corresponds to $Q(\rho_{\rm PPT})$. These two lines share a common point at $\alpha \approx 3.0669$. Except for this point, $U(\rho_{\rm PPT})$ is always larger than $Q(\rho_{\rm PPT})$ as we expect.

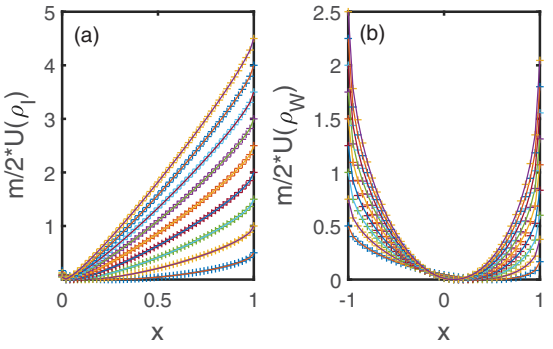

FIG. 3. Measurement-induced nonlocality $U(\rho_I)$ for the (a) isotropic states and (b) Werner states vs x. The solid line corresponds to the strictly analytical expression of Eq. (28) for (a) and Eq. (30) for (b), while the numerical expressions of Eq. (17) in both figures are marked by the +. The lines from bottom to top in both figures correspond to $m = 2,3,\ldots,10$.

with $N_T = \frac{5+\sqrt{25-4(383-34\sqrt{94})/9}}{2} \approx 3.0669$. Both the numerical result based on our theorem and the strictly analytic expression in Eq. (26) are plotted in Fig. 2(a) which shows the perfect consistency between them. In addition, we can analytically find the sudden change point of the measurement-induced nonlocality within the entanglement region. As a comparison, we also plot the local quantum uncertainty (LQU) $Q(\rho_{\rm PPT})$ given in Ref. [29] and the measurement-induced nonlocality $U(\rho_{\rm PPT})$ in Fig. 2(b). One can find that $U(\rho_{\rm PPT} = Q(\rho_{\rm PPT})$ at their common sudden change point and $U(\rho_{\rm PPT} > Q(\rho_{\rm PPT})$ as expected for other values of α.

4. $(m \otimes m)$-dimensional isotropic states

The isotropic states can be given by [67]

$$\rho_I = \frac{1-x}{m^2-1}\mathbb{I}_{m^2} + \frac{m^2x-1}{m^2-1}|\Phi\rangle\langle\Phi|, \quad x \in [-1,1], \tag{27}$$

with $|\Phi\rangle_m = \frac{1}{\sqrt{m}}\sum_{k=0}^{m-1}|kk\rangle$. Based on our definition, we can analytically obtain

$$U(\rho_I) = \frac{m^2x-2x+1-2\sqrt{x(1-x)(m^2-1)}}{m(1+m)}. \tag{28}$$

It is obvious that $U(\rho_I) = 0$ for $x = \frac{1}{m^2}$. As a comparison, we plot $U(\rho_I)$ given by Eqs. (17) and (28) in Fig. 3(a). The validity of our theorem is shown again.

5. $(m \otimes m)$-dimensional Werner states

The Werner states can be written as [67]

$$\rho_W = \frac{m-x}{m^3-m}\mathbb{I}_{m^2} + \frac{mx-1}{m^3-m}V, \quad x \in [-1,1], \tag{29}$$

with $V = \sum_{kl}|kl\rangle\langle lk|$ the swap operator. The measurement-induced nonlocality $U(\rho_W)$ in terms of our definition can given by

$$U(\rho_W) = \frac{m-x-\sqrt{(m^2-1)(1-x^2)}}{2(1+m)}. \tag{30}$$

From Eq. (30), it is shown that $U(\rho_W) = 0$ for $x = \frac{1}{m}$. The comparison between the numerical and the analytic expressions are given in Fig. 3(b) which again shows the perfect consistency.

Before the next example, we would like to emphasize that in both example 4 and example 5, the reduced density matrices ρ_A are the maximally mixed state which implies complete degeneracy. Intuitively, this belongs to the worst case mentioned in the last section (it requires the optimization in the total space of subsystem A). However, in the analytic procedure, one can find that all that are needed to be optimized can be automatically eliminated, which means no optimization is practically required. But it does not mean that the optimization is not performed in the numerical procedure. One can find that our numerical method stably approaches the unique optimal solution given in the analytic procedure. In this sense, the two examples provide more powerful proofs for the effectiveness of our theorem than other examples. In addition, considering the dual definitions of the measurement-induced nonlocality and LQU, one can find that $U = Q$ for both the isotropic states and the Werner states, since no optimization is practically covered, which is consistent with Ref. [68].

6. $(m \otimes m)$-dimensional degenerate and nondegenerate hybrid states

To demonstrate the practicability of our theorem and avoid the uniform degeneracy of the reduced density matrix, we construct a particular state as

$$\rho_H = \frac{\rho_W + P}{2} + \frac{(1-m+x)}{2(m^2-1)}(P - |11\rangle\langle 11|), \quad x \in [-1,1], \tag{31}$$

with $P = \frac{1}{n}\sum_{k=2}^{n+1}|kk\rangle\langle kk|$ and generally $m \geqslant 3$ and $n \in [2,m-1]$ to be supposed. The reduced density matrix ρ_A of this state has three different eigenvalues. Among them, there

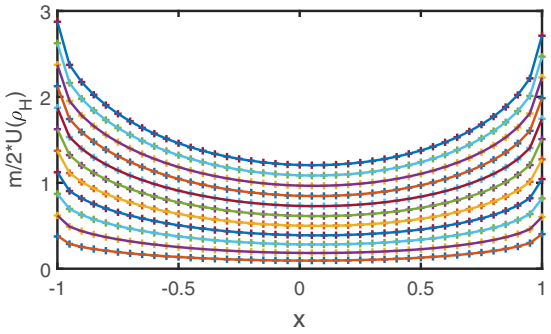

FIG. 4. Measurement-induced nonlocality $U(\rho_H)$ for hybrid states vs x. The solid line and the + line correspond to the strictly analytical expression of Eqs. (32) and (35) and the numerical expression of Eq. (17). The lines from bottom to top in the figure correspond to $m = 3,4,\ldots,13$.

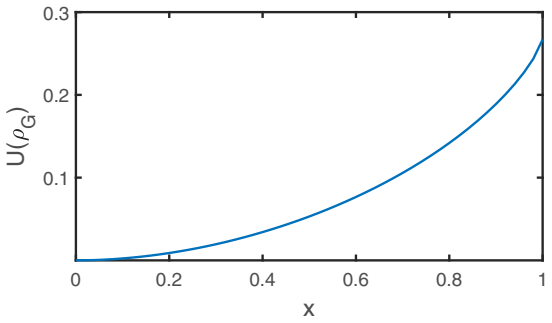

FIG. 5. Measurement-induced nonlocality $U(\rho_G)$ for general hybrid states vs x. The solid line corresponds to the numerical expression of Eq. (17).

could be two degenerate subspaces and one nondegenerate subspace. The eigenvalue $\frac{2m^2-mx-m-1}{2m(m^2-1)}$ is nondegenerate, the eigenvalue $\frac{m^3+mx-1}{2m(m^2-1)}$ is n-fold degenerate and the eigenvalue $\frac{1}{2m}$ is $(m-n-1)$-fold degenerate. However, one can note that if $m = 3$, then $n = 2$. Thus $(m-n-1) = 0$, i.e., this subspace corresponding to the eigenvalue $\frac{1}{2m}$ does not exist, which implies that the state has two different eigenvalues with only one degenerate subspace. When $m = 3$, one can find that the measurement-induced nonlocality $U(\rho_H)$ based on our definition is

$$U(\rho_H) = \frac{9 - 3x - 6\sqrt{2-2x^2} + (2-t)f(x)}{48}, \tag{32}$$

where

$$t = \begin{cases} m, & -1 < x \leqslant -\frac{14}{15}, \\ 1, & -\frac{14}{15} < x \leqslant 1, \end{cases} \tag{33}$$

and

$$f(x) = 11 + 3.5x - \sqrt{(7x+22)(x+1)} + 2\sqrt{2-2x^2} - \sqrt{(4x+44)(1-x)}. \tag{34}$$

When $m > 3$, the measurement-induced nonlocality $U(\rho_H)$ can be given by

$$U(\rho_H) = \frac{3}{4} - \frac{1}{4(m^3-m)}[2(m^2-x-1) + X_+(m-2n) + 2Y + (m^2-m-2n+2) \times \sqrt{X_+X_-} + (2n-2)\sqrt{X_+ + Y}(\sqrt{X_+} + \sqrt{X_-})], \tag{35}$$

where $X_\pm = (m \mp 1)(1 \pm x)$ and $Y = (m^2 + x - m)\frac{m}{n}$.

The comparison of the numerical and the analytic expressions is given in Fig. 4 which again shows perfect consistency.

7. General quantum states

To show the power of our theorem for high-dimensional states, we consider such a state ρ_G by mixing a maximally mixed state and a randomly generated (400×400)-dimensional mixed state G as

$$\rho_G = \frac{(1-x)}{400}\mathbb{I}_{400} + xG, \quad x \in [0,1]. \tag{36}$$

Since the matrix G is too large, it is impossible to explicitly give it here. The measurement-induced nonlocality versus x has been plotted in Fig. 5. We have uniformly taken 51 points in $x \in [0,1]$ and on average it takes about 8.4 s for the program (MATLAB R2014b) running on a personal laptop (2.8 GHz Intel Core i7/16 GB 1600 MHz DDR3).

V. CONCLUSIONS AND DISCUSSION

We have redefined the measurement-induced nonlocality based on the skew information associated with a broken observable instead of the original high-rank observable. This definition can solve the noncontractivity problem in the previous measurement-induced nonlocality based on the l_2 norm and has obvious operational meaning in terms of quantum metrology. It allows us to analytically calculate the measurement-induced nonlocality of pure states, qubit-qudit states, and some large classes of high-dimensional states. In particular, this definition enables us to develop the powerful inverse approximate joint diagonalization algorithm based on the very remarkable Jacobi method for the approximate joint diagonalization problem. It is shown that this inverse approximate joint diagonalization algorithm, similar to the corresponding approximate joint diagonalization algorithm, has good effectiveness because of its simplicity, stability, high efficiency, and state independence. This is further proven by the detailed comparisons between the analytic and numerical results of various examples. Compared with the diagonalization of a single density matrix, our measurement-induced nonlocality has even an almost-analytic expression for any quantum state, which gives an effective alternative means for the computability of the measurement-induced nonlocality.

Finally, we emphasize that the method applied to a broken observable is not a trivial skill but has many successful applications and can conquer many key problems in quantum discord and especially in quantum coherence. The potential application is worth our forthcoming attention. In addition, considering the quantum resource theory, it could be usually impossible for a general state to find an analytic quantifier of a general quantum resource, so how to develop an effective

numerical means should be a quite necessary problem. The power exhibited by the inverse approximate joint diagonalization and the approximate joint diagonalization algorithms could shed light on both the resource theory and other aspects of physics.

ACKNOWLEDGMENTS

This work was supported by the National Natural Science Foundation of China, under Grants No. 11775040 and No. 11375036, and the Xinghai Scholar Cultivation Plan.

[1] C. H. Bennett, H. J. Bernstein, S. Popescu, and B. Schumacher, Concentrating partial entanglement by local operations, Phys. Rev. A **53**, 2046 (1996).

[2] C. H. Bennett, D. P. DiVincenzo, J. A. Smolin, and W. K. Wootters, Mixed-state entanglement and quantum error correction, Phys. Rev. A **54**, 3824 (1996).

[3] C. H. Bennett, G. Brassard, S. Popescu, B. Schumacher, J. A. Smolin, and W. K. Wootters, Purification of Noisy Entanglement and Faithful Teleportation via Noisy Channels, Phys. Rev. Lett. **76**, 722 (1996).

[4] P. Horodecki and R. Horodecki, Distillation and bound entanglement, Quant. Inf. Comp. **1**, 45 (2001).

[5] W. K. Wootters, Entanglement of formation and concurrence, Quant. Inf. Comp. **1**, 27 (2001).

[6] R. Horodecki, P. Horodecki, M. Horodecki, and K. Horodecki, Quantum entanglement, Rev. Mod. Phys. **81**, 865 (2009).

[7] L. Henderson and V. Vedral, Classical, quantum and total correlations, J. Phys. A: Math. Theor. **34**, 6899 (2001).

[8] H. Ollivier, W. H. Zurek, Quantum Discord: A Measure of the Quantumness of Correlations, Phys. Rev. Lett. **88**, 017901 (2001).

[9] A. Datta, A. Shaji, and C. M. Caves, Quantum Discord and the Power of One Qubit, Phys. Rev. Lett. **100**, 050502 (2008).

[10] T. Tufarelli, D. Girolami, R. Vasile, S. Bose, and G. Adesso, Quantum resources for hybrid communication via qubit-oscillator states, Phys. Rev. A **86**, 052326 (2012).

[11] C. S. Yu, J. Zhang, and H. Fan, Quantum dissonance is rejected in an overlap measurement scheme, Phys. Rev. A **86**, 052317 (2012).

[12] A. Brodutch, Discord and quantum computational resources, Phys. Rev. A **88**, 022307 (2013).

[13] T. Baumgratz, M. Cramer, and M. B. Plenio, Quantifying Coherence, Phys. Rev. Lett. **113**, 140401 (2014).

[14] A. Winter and D. Yang, Operational Resource Theory of Coherence, Phys. Rev. Lett. **116**, 120404 (2016).

[15] E. Chitambar and M. H. Hsieh, Relating the Resource Theories of Entanglement and Quantum Coherence, Phys. Rev. Lett. **117**, 020402 (2016).

[16] A. Streltsov, S. Rana, P. Boes, and J. Eisert, Structure of the Resource Theory of Quantum Coherence, Phys. Rev. Lett. **119**, 140402 (2017).

[17] K. B. Dana, M. G. Díaz, M. Mejatty, and A. Winter, Resource theory of coherence: Beyond states, Phys. Rev. A **95**, 062327 (2017).

[18] A. Streltsov, S. Rana, M. N. Bera, and M. Lewenstein, Towards resource theory of coherence in distributed scenarios, Phys. Rev. X **7**, 011024 (2017).

[19] F. G. S. L. Brandão, M. Horodecki, J. Oppenheim, J. M. Renes, and R. W. Spekkens, Resource Theory of Quantum States Out of Thermal Equilibrium, Phys. Rev. Lett. **111**, 250404 (2013).

[20] F. G. S. L. Brandão and G. Gour, Reversible Framework for Quantum Resource Theories, Phys. Rev. Lett. **115**, 070503 (2015).

[21] C. S. Yu, Quantum coherence via skew information and its polygamy, Phys. Rev. A **95**, 042337 (2017).

[22] A. Peres, Separability Criterion for Density Matrices, Phys. Rev. Lett. **77**, 1413 (1996).

[23] W. K. Wootters, Entanglement of Formation of An Arbitrary State of Two Qubits, Phys. Rev. Lett. **80**, 2245 (1998).

[24] G. Vidal, and R. F. Werner, Computable measure of entanglement, Phys. Rev. A **65**, 032314 (2002).

[25] S. L. Luo, Quantum discord for two-qubit systems, Phys. Rev. A **77**, 042303 (2008).

[26] S. L. Luo, Using measurement-induced disturbance to characterize correlations as classical or quantum, Phys. Rev. A **77**, 022301 (2008).

[27] B. Dakić, V. Vedral, and Č. Brukner, Necessary and Sufficient Condition for Nonzero Quantum Discord, Phys. Rev. Lett. **105**, 190502 (2010).

[28] D. Girolami, T. Tufarelli, and G. Adesso, Characterizing Nonclassical Correlations Via Local Quantum Uncertainty, Phys. Rev. Lett. **110**, 240402 (2013).

[29] C. S. Yu, S. X. Wu, X. G. Wang, X. X. Yi, and H. S. Song, Quantum correlation measure in arbitrary bipartite systems, Europhys. Lett. **107**, 10007 (2017).

[30] F. Mintert, M. Kuś, and A. Buchleitner, Concurrence of Mixed Bipartite Quantum States in Arbitrary Dimensions, Phys. Rev. Lett. **92**, 167902 (2004).

[31] K. Chen, S. Albeverio, and S. M. Fei, Concurrence of Arbitrary Dimensional Bipartite Quantum States, Phys. Rev. Lett. **95**, 040504 (2005).

[32] C. S. Yu and H. S. Song, Separability criterion of tripartite qubit systems, Phys. Rev. A **72**, 022333 (2005).

[33] K. Audenaert, F. Verstraete, and B. D. Moor, Variational characterizations of separability and entanglement of formation, Phys. Rev. A **64**, 052304 (2001).

[34] M. A. Jafarizadenh, M. Mirzaee, and M. Rezaee, Best separable approximation with semi-definite programming method, Int. J. Quant. Inf. **2**, 541 (2004).

[35] J. Řeháček and Z. Hradil, Quantification of Entanglement by Means of Convergent Iterations, Phys. Rev. Lett. **90**, 127904 (2003).

[36] Y. Zinchenko, S. Friedland, and G. Gour, Numerical estimation of the relative entropy of entanglement, Phys. Rev. A **82**, 052336 (2010).

[37] K. Cao, Z. W. Zhou, G. C. Guo, and L. X. He, Efficient numerical method to calculate the three-tangle of mixed states, Phys. Rev. A **81**, 034302 (2010).

[38] B. Röthlisberger, J. Lehmann, and D. Loss, Comp. Phys. Commun. **183**, 155 (2012).

[39] B. Röthlisberger, J. Lehmann, D. S. Saraga, P. Traber, and D. Loss, Highly Entangled Ground States in Tripartite Qubit Systems, Phys. Rev. Lett. **100**, 100502 (2008).

[40] B. Röthlisberger, J. Lehmann, and D. Loss, Numerical evaluation of convex-roof entanglement measures with applications to spin rings, Phys. Rev. A **80**, 042301 (2009).

[41] C. Napoli, T. R. Bromley, M. Cianciaruso, M. Piani, N. Johnston, and G. Adesso, Robustness of Coherence: An Operational and Observable Measure of Quantum Coherence, Phys. Rev. Lett. **116**, 150502 (2016).

[42] M. Piani, M. Cianciaruso, T. R. Bromley, C. Napoli, N. Johnston, and G. Adesso, Robustness of asymmetry and coherence of quantum states, Phys. Rev. A **93**, 042107 (2016).

[43] S. Rana, P. Parashar, and M. Lewenstein, Trace-distance measure of coherence, Phys. Rev. A **93**, 012110 (2016).

[44] P. Zanardi, G. Styliaris, and L. C. Venuti, Measures of coherence-generating power for quantum unital operations, Phys. Rev. A **95**, 052307 (2017).

[45] S. L. Luo and S. S. Fu, Measurement-Induced Nonlocality, Phys. Rev. Lett. **106**, 120401 (2011).

[46] S. L. Luo, and S. S. Fu, Geometric measure of quantum discord, Phys. Rev. A **82**, 034302 (2010).

[47] M. Piani, Problem with geometric discord, Phys. Rev. A **86**, 034101 (2012).

[48] S. Y. Mirafzali, I. Sargolzahi, A. Ahanj, K. Javidan, and M. Sarbishaei, Measurement-induced nonlocality for an arbitrary bipartite state, Quant. Inf. Comp. **1**, 0479 (2013).

[49] A. Sen, D. Sarkar, and A. Bhar, Monogamy of measurement-induced nonlocality, J. Phys. A Math. Theor., **45**, 405306 (2012).

[50] S. Rana, and P. Parashar, Geometric discord and measurement-induced nonlocality for well known bound entangled states, Quant. Inf. Proc. **12**, 2523 (2013).

[51] S. X. Wu, J. Zhang, C. S. Yu, and H. S. Song, Uncertainty-induced quantum nonlocality, Phys. Letts. A **378**, 344 (2014).

[52] M. L. Hu and H. Fan, Measurement-induced nonlocality based on the trace norm, New. J. Phys. **17**, 033004 (2015).

[53] L. D. Wang, L. T. Wang, M. Yang, J. Z. Xu, Z. D. Wang, and Y. K. Bai, Entanglement and measurement-induced nonlocality of mixed maximally entangled states in multipartite dynamics, Phys. Rev. A **93**, 062309 (2016).

[54] Z. J. Xi, X. G. Wang, and Y. M. Li, Measurement-induced nonlocality based on the relative entropy, Phys. Rev. A **85**, 042325 (2012).

[55] E. P. Wiger and M. M. Yanase, Information contents of distributions, Proc. Natl. Acad. Sci. USA, **49**, 910 (1963).

[56] E. H. Lieb, Convex trace functions and the Wigner-Yanase-Dyson conjecture, Adv. Math. **11**, 267 (1973).

[57] S. L. Luo, Wigner-Yanase Skew Information and Uncertainty Relations, Phys. Rev. Lett. **91**, 180403 (2003).

[58] U. Dorner, R. Demkowicz-Dobrzanski, B. J. Smith, J. S. Lundeen, W. Wasilewski, K. Banaszek, and I. A. Walmsley, Optimal Quantum Phase Estimation, Phys. Rev. Lett. **102**, 040403 (2009).

[59] S. L. Braunstein and C. M. Caves, Statistical Distance and the Geometry of Quantum States, Phys. Rev. Lett. **72**, 3439 (1994).

[60] S. L. Braunstein, C. M. Caves, and G. J. Milburn, Generalized uncertainty relations: Theory, examples, and Lorentz invariance, Ann. Phys. (NY) **247**, 135 (1996).

[61] S. L. Luo, Wigner-Yanase skew information vs. quantum Fisher information, Proc. Am. Math. Soc. **132**, 885 (2003).

[62] J. F. Cordoso and A. Souloumiac, Blind beam forming for non-Gaussian signals, Radar Signal Process, IEE Proceedings-F **140**, 362 (1993).

[63] J. F. Cordoso and A. Souloumiac, Jacobo angles for simultaneous diagonalization, SIAM J. Mater. Anal. Appl. **17**, 161 (1996).

[64] A. Ziehe, P. Laskov, G. Nolte, and K. R. Müller, A fast algorithm for joint diagonalization with nonorthogonal transformations and its application to blind source separation, J. Mach. Learn. Res. **5**, 777 (2004).

[65] G. H. Golub and C. F. Van Loan, *Matrix Computations*, 3rd ed. (Johns Hopkins University, Baltimore, 1996).

[66] C. F. Van Loan and N. P. Pitsianis, *Linear Algebra for Large Scale and Real Time Applications*, edited by M. S. Moonen and G. H. Golub (Kluwer, Dordrecht, 1993), pp. 293–314.

[67] G. Alber, T. Beth, M. Horodecki, P. Horodecki, R. Horodecki, M. Rötteler, H. Weinfurter, R. Werner, and A. Zeilinger, *Quantum Information: An Introduction to Basic Theoretical Concepts and Experiments* (Springer-Verlag, Berlin, 2001).

[68] L. N. Chang and S. L. Luo, Remedying the local ancilla problem with geometric discord, Phys. Rev. A **87**, 062303 (2013).